EXPERIMENTAL PROCEDURES

Isothermal titration calorimetry (ITC). ITC measurements were carried out using a MicroCal VP-ITC instrument (Northampton, MA). The sample cell (1.43 mL) contained 5-10 μM apoferritin 24-mer in 130 mM NaCl, 20 mM NaHPO4, pH 7.0, and the reference cell contained water. Ligands were solubilized in the same buffer as the protein. All ligands (except phenol and 2-ethyl-6-methylphenol) were prepared as saturated solutions by adding excess ligand to buffer, followed by vigorous vortexing and sonication and then filtration through 0.2 μm PTFE syringe filters. Concentrations were then measured by UV absorbance. Concentrations of ligand in the syringe ranged from 0.07-23.4 mM. Each ligand was titrated into the sample cell from a syringe containing 286 μL of ligand solution. The titration volumes were 1 μL volume for the first injection and 15 μL volumes thereafter, with 5 min intervals between injections. The experiments were performed at 20 °C. The data were corrected for heats of dilution using titrations of ligand into buffer, buffer into protein, and buffer into buffer.

The enthalpy data were fit to a model using a single set of independent sites using *Origin 5.0* (Microcal, Inc). The stoichiometry predicted by the fits ranged from 0.9 to 3.6 binding sites per apoferritin 24-mer, depending on the ligand. For the two ligands with the weakest affinities, dimethylphenol and phenol, the estimated error in stoichiometry was large, and so this value was forced to 1 per 24-mer. All measurements were carried out at least in duplicate and the resultant K_a values were averaged for each ligand (Table 2).

Protein Crystallization. Large oligomers (>24-mer) were removed from the apoferritin preparation by gel filtration chromatography on a Sephacryl S-300 column, using 0.2 M NaOAc pH 5.0 as the mobile phase (1). The fractions corresponding to apoferritin 24-mer were pooled and concentrated to 12 mg/mL and used for co-crystallization experiments. Unpurified apoferritin was used for crystallization of unliganded protein.

Apoferritin was crystallized using the hanging drop vapor diffusion method at 18 °C, using a drop containing 1 μL of the protein solution plus 1 μL of the reservoir solution equilibrated over 1 mL of reservoir. The reservoir contained an unbuffered solution of ammonium sulfate and cadmium sulfate. Typically, a grid covering the range 0.2-1.2 M $(NH_4)_2SO_4$ and 0.1-0.225 M $CdSO_4$ was searched; crystals appeared thoughout this grid, but for any given experiment the precise conditions yielding the best large single crystals might lie anywhere in this grid. For co-crystallization experiments, the ligand was added to both the reservoir and the protein solution at a final concentration of 1 mM (5 mM for phenol). Crystals grew to a final size of 200-400 μm in one to two weeks. Prior to data collection, crystals were captured in nylon loops, briefly dipped into a cryoprotectant solution containing ligand (7 volumes reservoir solution plus 3 volumes glycerol), and flash cooled in liquid nitrogen.

Data Processing and Refinement. Diffraction data were collected at beamlines X6A and X25 of the National Synchrotron Light Source and 17-ID of the Advanced Photon Source. Crystals were maintained at 100 K during data collection. Data were integrated and merged using the program d*TREK97 (2). The structures were determined using the difference Fourier technique using 1XZ1 as the starting model. The programs REFMAC5 (3) and Coot (4) were used in refinement and rebuilding, respectively. Simulated annealing as implemented in CNS was used to remove model bias after initial rigid body refinement (5). Water molecules were found using ARP/wARP in the CCP4 suite (6). Only waters that had peaks in both Fo-Fc and 2Fo-Fc maps and were within hydrogen bonding distance to polar atoms in the protein or other perceived waters were retained for further refinement. Cd (II) ions were modeled with the aid of anomalous difference maps. Representative electron density is shown in Figure S2 for the different ligand complexes.

Volume calculations. Cavity and ligand volumes were calculated using VOIDOO (7). All ligand complexes were superposed on the unliganded apoferritin structure using lsqman (8) before volume analysis. Van der Waals volumes of the ligands were calculated using a primary grid spacing of 0.5 Å and probe radius = 0. The probe-occupied cavity volumes were calculated using a probe size of 1.4 Å and primary grid spacing of 0.5 Å. For each of the complexes, volumes were determined for ten random orientations and the

results were averaged. The volumes were refined for 25 cycles or until consecutive volumes converged to <0.05 %. Packing densities were calculated as the ratio of ligand volume to cavity volume.

The anesthetic-binding cavity is connected to the protein surface by two small openings, the sizes of which are acutely sensitive to slight conformational changes in the "gatekeeper" Arg-59 residues. In some structures the cavity is fully enclosed, i.e. the openings are smaller than the volume probe, while in others the openings are enlarged slightly, allowing the probe to escape the cavity and leading to erroneously large calculated cavity volumes. To overcome this problem, the cavity generated by VOIDOO was filled with water molecules using FLOOD (7). The water molecules lying just outside the cavity, closest to the narrowest point of the cavity mouth, were appended to the original coordinate file and VOIDOO was re-run. These waters act as "stoppers" to provide an objective cavity boundary at the pinch-point formed by the cavity mouth. To ensure that this procedure did not give rise to any artifactual volume differences between different complex structures, the same water molecules found by FLOOD for the apoferritin-propofol complex were appended to *all* coordinate files for volume calculations.

The cavity in which anesthetics bind lies at the interface between two apoferritin monomers, which are related by a crystallographic 2-fold axis that passes through the center of the cavity. Hence, each ligand exhibits two-fold disorder, with the maximum possible occupancy for each ligand position being 0.5. It is possible that the actual occupancy for some ligands is lower than this value; however, in the absence of extremely high resolution data it is notoriously difficult to robustly refine occupancies, and for this reason the ligand occupancies were set at 0.5 and not refined. Three side chains that line the cavity, Ser-27, Arg-59, and Leu-81, exhibit alternate conformations in the presence of some of the ligands. Typically, only one of the two alternate conformers is sterically compatible with a particular ligand position. This conformer was used for volume calculations.

Molecular dynamics. Simulation systems were generated by placing an apoferritin dimer in a truncated octahedral water box generated using the SOLVATE feature of VMD (9). The geometry and size of the water box (about 18,000 water molecules in a box with a largest dimension of 97 Å) were chosen to ensure that the protein would not interact with its periodic images, even upon rotation of the dimer or extension of the loop regions. Na^+ and Cl^- ions were added using the IONIZE feature of VMD to obtain a 0.15 M neutral solution. The three systems contained either no ligand (control), phenol, or propofol bound in the cavity, in the orientations indicated by the crystal structures. Total system size ranged from 58,375 to 58,568 atoms for the three systems. The propofol system was simulated twice, under two distinct equilibration protocols, as described below.

Simulations were conducted using the molecular dynamics package NAMD (10). All simulations underwent 1000 steps of energy minimization. The control and phenol simulations, and one of the propofol simulations (propofol-A), were then equilibrated by restraining the protein C_a carbons to their initial positions with a harmonic force of 2.0 kcal/mol/Å^2 for a total of 500 ps, followed by simulation with no restraints. The second propofol system (propofol-B) was equilibrated more slowly in a protocol that restrained the ligand as well as the α-carbons: for the first 3 ns the α-carbons and the ligand atoms were restrained to their initial positions with a harmonic force of 4 kcal/mol/Å^2, followed by 1 ns in which the harmonic force was 2 kcal/mol/Å^2, followed by 1 ns in which the harmonic force was 1 kcal/mol/Å^2, followed by unrestrained simulation. The propofol-A simulation was run for a total of 40 ns, while the propofol-B, phenol, and control simulations were run for a total of 20 ns. Hydrogen bonding was assessed over the course of the different simulations, using a distance cutoff of 3.3 Å and an angle cutoff of 25°.

The CHARMM27 forcefield (11) was used for protein parameters, the parameters of Beglov and Roux (12) governed ions, and the system was solvated by TIP3P(13) waters. The CHARMM27 forcefield also provides parameters for phenol, and parameters for propofol were determined using the CHARMM27 parameters for phenol and isopropyl groups. The dihedral potential that governs rotation of the isopropyl moiety of propofol with respect to the central ring is not specified in the CHARMM27 potential but was set to vanish, as a quantum-mechanical dihedral scan conducted using

GAUSSIAN (14) indicated that 1-4 interactions alone resulted in a sufficiently high rotation barrier.

Energy minimization and molecular dynamics simulations were conducted using NAMD2 (15). All simulations used periodic boundary conditions and particle-mesh Ewald for long-range electrostatics. Lennard-Jones potentials were truncated at 1.2 nm, with a smooth switching function starting at 1.0 nm. Bonds to hydrogen atoms were constrained to their equilibrium length with RATTLE. Multiple-timestep integration was carried out using r-RESPA, with a base time step of 2 fs and a secondary time step of 4 fs for long-range interactions. A Langevin thermostat maintained a constant temperature of 300 K and a Langevin piston maintained a constant isotropic pressure of 1 bar.

REFERENCES

1. Thomas, B. R., Carter, D., and Rosenberger, F. (1998) *J. Crystal Growth* **187**, 499-510
2. Pflugrath, J. W. (1999) *Acta Crystallogr. D Biol. Crystallogr.* **D55**, 1718-1725
3. Murshudov, G. N., Vagin, A. A., and Dodson, E. J. (1997) *Acta Crystallogr. D Biol. Crystallogr.* **D53**, 240-255
4. Emsley, P., and Cowtan, K. (2004) *Acta Crystallogr. D Biol. Crystallogr.* **D60**, 2126-2132
5. Brünger, A. T., Adams, P. D., Clore, G. M., Gros, P., Grosse-Kunstleve, R. W., Jiang, J.-S., Kuszewski, J., Nilges, N., Pannu, N. S., Read, R. J., Rice, L. M., Simonson, T., and Warren, G. L. (1998) *Acta Crystallogr. D Biol. Crystallogr.* **D54**, 905-921
6. Lamzin, V. S., Perrakis, A., and Wilson, K. S. (2001) The ARP/wARP suite for automated construction and refinement of protein models. in *International Tables for Crystallography, Vol. F. Crystallography of Biological Macromolecules* (Rossmann, M. G., and Arnold, E. eds.), Kluwer Academic Publishers, The Netherlands
7. Kleywegt, G. J., and Jones, T. A. (1994) *Acta Crystallogr. D Biol. Crystallogr.* **D50**, 178-185
8. Kleywegt, G. J., Zou, J. Y., Kjeldgaard, M., and Jones, T. A. (2001) Around O. in *International Tables for Crystallography, Vol. F. Crystallography of Biological Macromolecules* (Rossmann, M. G., and Arnold, E. eds.), Dordrecht: Kluwer Academic Publishers, The Netherlands
9. Humphrey, W., Dalke, A., and Schulten, K. (1996) *J. Mol. Graph.* **14**, 33-38
10. Phillips, J. C., Braun, R., Wang, W., Gumbart, J., Tajkhorshid, E., Villa, E., Chipot, C., Skeel, R. D., Kale, L., and Shulten, K. (2005) *J Comput Chem* **26**, 1781-1802
11. MacKerell, A., Bashford, D., Bellott, M., Dunbrack Jr., R. L., Evansec, J. D., Field, M. J., Fischer, S., Guo, H., Ha, S., Joseph-McCarthy, D., Kuchnir, L., Kuczera, K., Lau, F. T. K., Mattos, C., Michnick, S., Ngo, T., Nguyen, D. T., Prodhom, B., Reiher III, W. E., Roux, B., Schlenkrich, M., Smith, J. C., Stote, R., Straub, J., M., W., Wiorkiewicz-Kuczera, J., Yin, D., and Karplus, M. (1998) *J. Phys. Chem. B.* **102**, 3586-3616
12. Beglov, D., and Roux, B. (1994) *J. Chem. Phys.* **100**, 9050-9063
13. Jorgensen, W. L., Chandrasekhar, J., Madura, J. D., Impey, R. W., and Klein, M. L. (1983) *J. Chem. Phys.* **79**, 926-935
14. Frisch, M. J., Trucks, G. W., Schlegel, H. B., Scuseria, G. E., Robb, M. A., Cheeseman, J. R., Montgomery Jr., J. A., Vreven, T., Kudin, K. N., Burant, J. C., Millam, J. M., Iyengar, S. S., Tomasi, J., Barone, V., Mennucci, B., Cossi, M., Scalmani, G., Rega, N., Petersson, G. A., Nakatsuji, H., Hada, M., Ehara, M., Toyota, K., Fukuda, R., Hasegawa, J., Ishida, M., Nakajima, T., Honda, Y., Kitao, O., Nakai, H., Klene, M., Li, X., Knox, J. E., Hratchian, H. P., Cross, J. B., Bakken, V., Adamo, C., Jaramillo, J., Gomperts, R., Stratmann, R. E., Yazyev, O., Austin, A. J., Cammi, R., Pomelli, C., Ochterski, J. W., Ayala, P. Y., Morokuma, K., Voth, G. A., Salvador, P., Dannenberg, J. J., Zakrzewski, V. G., Dapprich, S., Daniels, A. D., Strain, M. C., Farkas, O., Malick, D. K., Rabuck, A. D., Raghavachari, K., Foresman, J. B., Ortiz, J. V., Cui, Q., Baboul, A. G., Clifford, S., Cioslowski, J., Stefanov, B. B., Liu, G., Liashenko, A., Piskorz, P., Komaromi, I., Martin, R. L., Fox, D. J., Keith, T., Al-Laham, M. A., Peng, C. Y., Nanayakkara, A.,

Challacombe, M., Gill, P. M. W., Johnson, B., Chen, W., Wong, M. W., Gonzalez, C., and Pople, J. A. (2004) Gaussian 03, Revision C.02. Gaussian, Inc., Wallingford, CT

15. Kalé, L., Skeel, R., Bhandarkar, M., Brunner, R., Gursoy, A., Krawetz, N., Phillips, J., Shinozaki, A., Varadarajan, K., and Schulten, K. (1999) *J. Comp. Phys.* **151**, 283-312

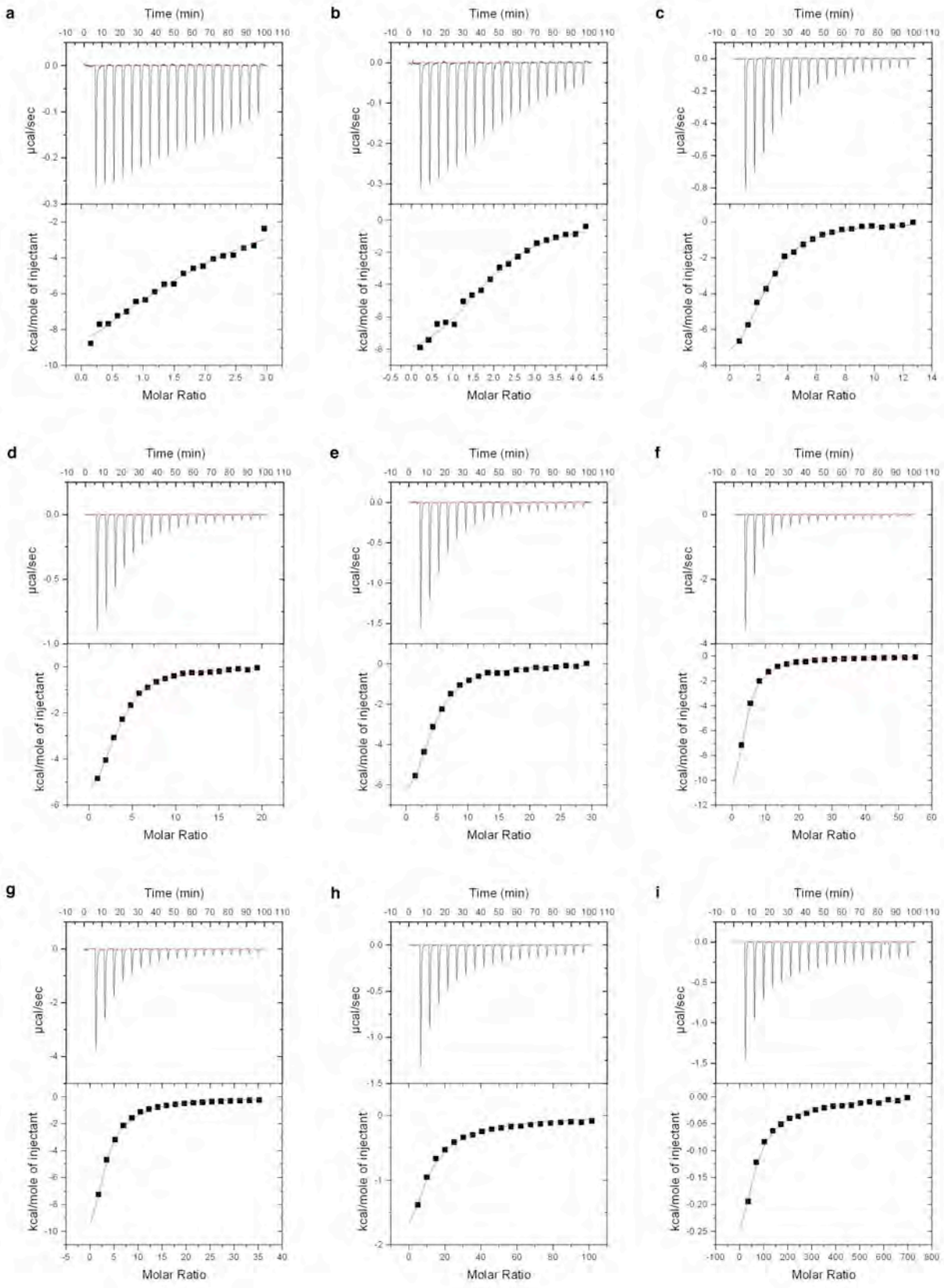
a
b
c
d
e
f
g
h
i
Time (min)
µcal/sec
kcal/mole of injectant
Molar Ratio

Fig. S1 (preceding page): Isothermal calorimetry titrations of apoferritin with propofol and its analogues. Upper panels show representative enthalpograms and lower panels show a single class binding site fit to the data. (a) 0.07 mM 2,6-di-sec-butylphenol (compound **2**) ; (b) 0.1 mM 2-sec-butyl-6-isopropylphenol (compound **3**) ; (c) 0.3 mM 2-isopropyl-6-propylphenol (compound **4**); (d) 0.46 mM 2,6-diisopropylphenol (propofol, compound **1**); (e) 0.69 mM 2,6-diethylphenol (compound **5**); (f) 1.3 mM 2-isopropylphenol (compound **7**); (g) 1.6 mM 2-ethyl-6-methylphenol (compound **6**); (h) 2.4 mM 2,6-dimethylphenol (compound **8**); (i) 16.5 mM phenol (compound **9**). Apoferritin concentrations fall in the range 5-10 μM.

Fig. S2 (below and following pages): Stereo views of representative 2Fo – Fc electron density for the different apoferritin-ligand complexes. The same portion of the molecule that is shown in Figure 2 is shown here, with the superimposed electron density contoured at 1σ.

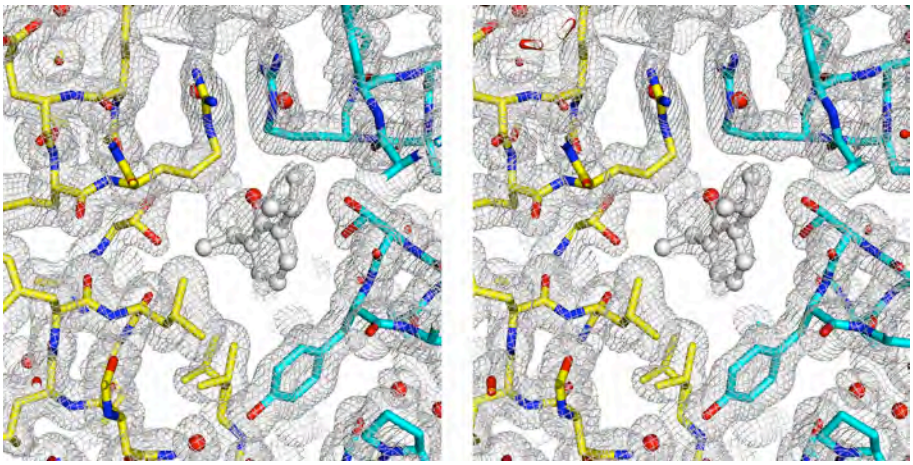

propofol (**1**)

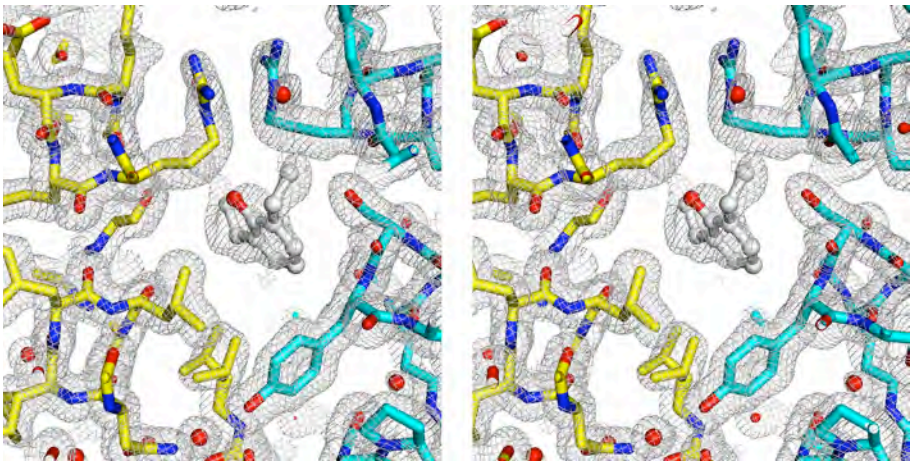

2,6-diethylphenol (**5**)

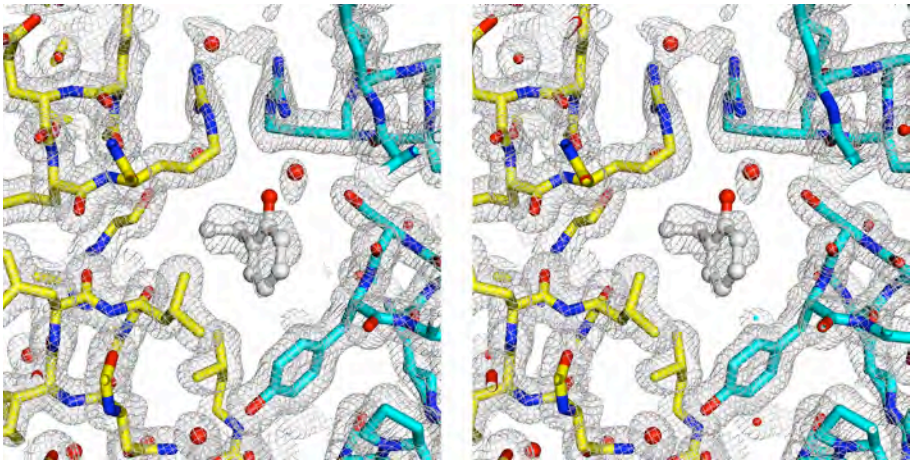

2-isopropylphenol (**7**)

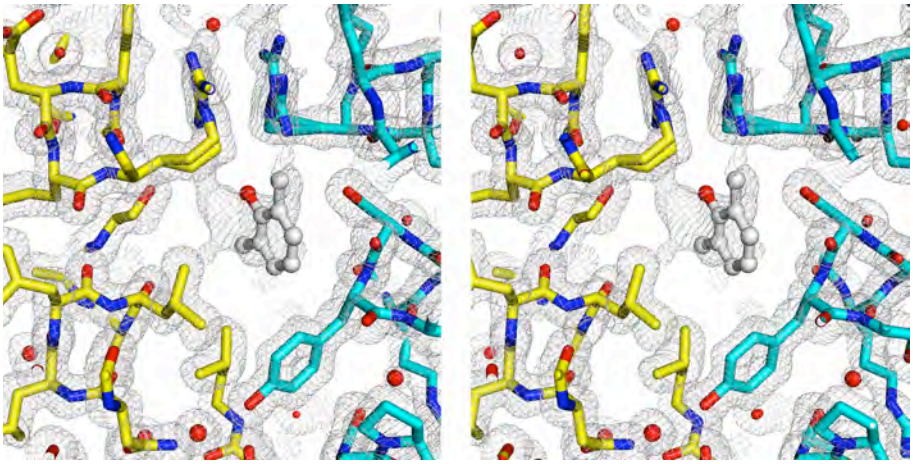

2,6-dimethylphenol (**8**)

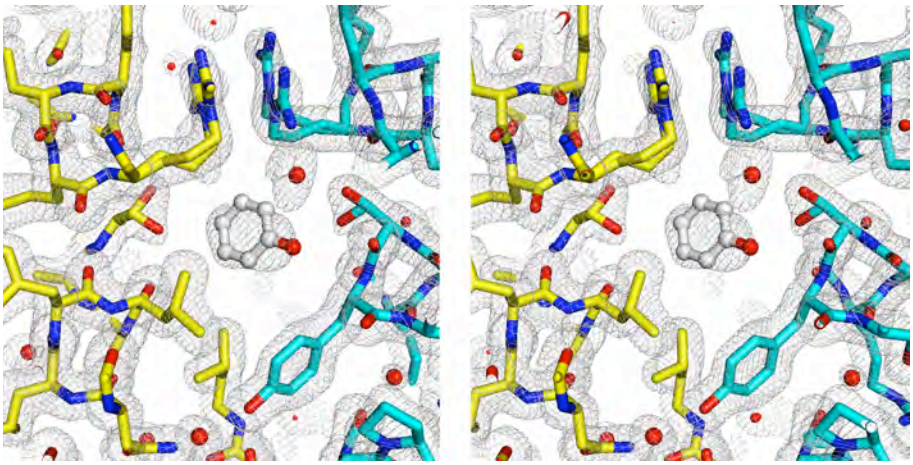

phenol (**9**)